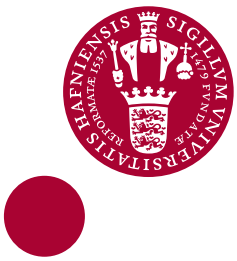

Molecular Dynamics Simulations Reveal the Proton:Peptide Coupling Mechanism in the Bacterial Proton-Coupled Oligopeptide Transporter YbgH

Aduri, Nanda G.; Montefiori, Marco; Khalil, Ruqaiya; Gajhede, Michael; Jørgensen, Flemming Steen; Mirza, Osman

Published in:
ACS Omega

DOI:
10.1021/acsomega.8b02131

Publication date:
2019

Document version
Publisher's PDF, also known as Version of record

ACS OMEGA

Article

Cite This: ACS Omega 2019, 4, 2040−2046

http://pubs.acs.org/journal/acsodf

Molecular Dynamics Simulations Reveal the Proton:Peptide Coupling Mechanism in the Bacterial Proton-Coupled Oligopeptide Transporter YbgH

Nanda G. Aduri,[†] Marco Montefiori,[†] Ruqaiya Khalil,[‡] Michael Gajhede,[†] Flemming Steen Jørgensen,[†] and Osman Mirza*[,†]

[†]Department of Drug Design and Pharmacology, Faculty of Health and Medical Sciences, University of Copenhagen, Copenhagen DK-2100, Denmark

[‡]Dr. Panjwani Center for Molecular Medicine and Drug Research, International Center for Chemical and Biological Sciences, University of Karachi, Karachi 75270, Pakistan

ABSTRACT: Proton-coupled oligopeptide transporters (POTs) couple the inward movement of di- or tripeptides with the inward movement of protons. Experimentally, it has been shown that virtually all di- and tripeptides are recognized as substrates, which suggests that it is the backbone of the peptide that determines substrate affinity and specificity. We have previously shown that a conserved E_1XXE_2R motif is involved in the binding of the proton. Although the proposed protonation site is in close proximity to the peptide binding site, the mechanism by which the POTs couple protonation to peptide binding is not understood. Here, we have performed molecular dynamics simulations on the crystal structure of *Escherichia coli* POT YbgH in the absence and presence of a proton on the consensus E_2 (Glu21) and on both states in the absence and presence of a dipeptide. We observe that the highly conserved Lys118 is able to interact with Glu21 when Glu21 is not protonated but with the dipeptide C-terminus when Glu21 is protonated. Thus, Lys118 provides YbgH with a coupling mechanism sensor that ensures detection of protonation and peptide binding. Furthermore, we observe that the dipeptide initially interacts only with Glu391, with the rest of the peptide being flexible, and becomes stabilized upon interaction with Lys118. This suggests that the peptide binding is a two-step procedure and that the transition from the first to the second step depends upon protonation of Glu21. Finally, we observe occluded conformations of YbgH during the simulations. Most strikingly, in YbgH devoid of peptide, the highly conserved residues Tyr26 and Arg29 interact with Glu391, overlapping with the space that would otherwise be occupied by a bound peptide. This intramolecular substrate mimicry may explain how the apo transporter returns back into the outside-facing conformation.

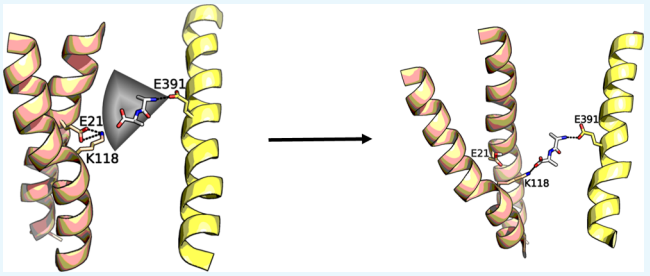

INTRODUCTION

Proton-coupled transporters are able to utilize the electrochemical proton gradient to facilitate uphill transport of solutes such as sugars, amino acids, vitamins, and peptides. A significant number of these symporters belong to the major facilitator superfamily (MFS), which contains over 100 transporter families. The overall structure of MFS transporters consists of two interconnected 6-helix domains. In spite of having the same overall fold, the MFS transporters utilize the structural framework very differently to recognize distinct substrate molecules, and the mechanism by which the proton electrochemical gradient is utilized also seems to differ substantially.[1]

The proton-coupled oligopeptide transporter (POT) family transports almost all types of di- and tripeptides along with energizing protons.[2−4] Several crystal structures of POT members from different bacterial species, with and without bound peptides, have been determined so far, laying the foundation for rational mutagenic studies as well as computational experiments.[5] Site-directed mutagenesis of a number of residues in the substrate binding site of POTs have pinpointed those residues that most likely play a role in proton or peptide binding or in both.[2−4,6−16] The consensus from these studies is that the so-called E_1XXE_2R motif present in helix I is responsible for binding of the proton[13,16] and that a tyrosine (helix I) and a glutamate (helix X) interact with the peptide backbone and N-terminus, respectively.[2−4] A lysine on helix IV interacts with the peptide C-terminus[2,4,7] and has also been suggested to interact with E_1 following protonation of E_2.[11] Protonation of E_2 has also been suggested to prompt overall structural changes.

The POT from *Geobacillus kaustophilus* (GkPOT) has been crystallized and subsequently studied by molecular dynamics

Received: August 22, 2018
Accepted: December 11, 2018
Published: January 25, 2019

DOI: 10.1021/acsomega.8b02131
ACS Omega 2019, 4, 2040−2046

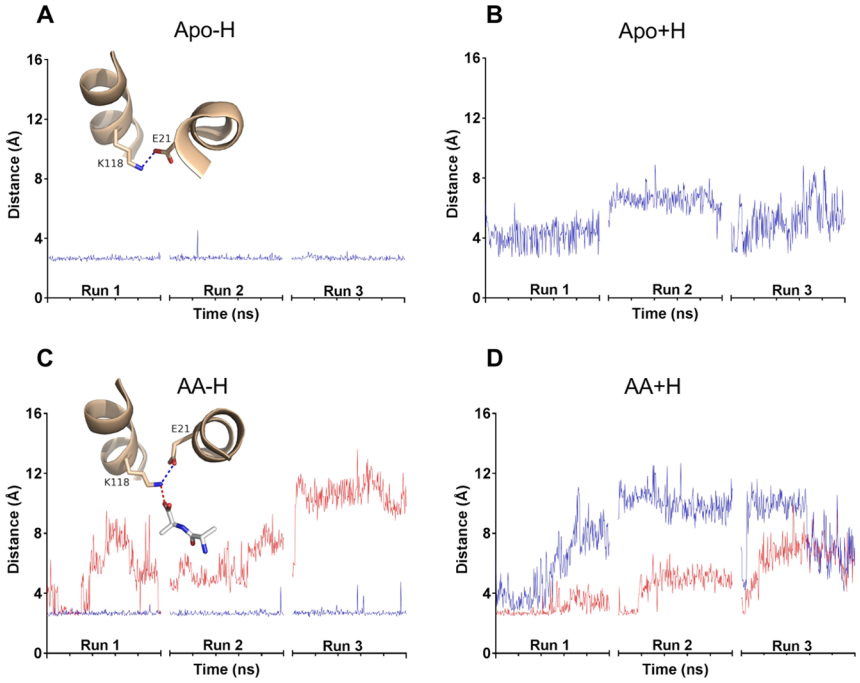

Figure 1. Influence of protonation on Glu21 on Lys118 and Ala−Ala C-terminal interactions. The shortest side chain N−O distance (Å) from Lys118 to Glu21 (blue) and Ala−Ala C-terminal (red) as a function of time in (A) apo−H, (B) apo+H, (C) AA−H, and (D) AA+H. Each run segment corresponds to 100 ns. Insets represent the bond distances that were measured, where Ala−Ala is shown with white carbon atoms and YbgH residue carbon atoms in wheat color.

(MD) calculations.[17,18] Here, a glutamate on helix VII (Glu310) is found to be the site of protonation.

YbgH and YjdL are homologous POTs from *Escherichia coli* that have the same uncommon E_1XXE_2R motif with the E_1 position being a glutamine and the R position a tyrosine residue. In addition, the GkPOT Glu310 equivalent is a glutamine and can therefore be excluded as the site of protonation. Despite this, they are able to transport peptides in a proton-dependent manner, just like *E. coli* YdgR and YhiP, which both contain an intact E_1XXE_2R motif.[10,16] The crystal structure of YbgH was determined recently,[16] and although the structure of YjdL is yet not determined, YjdL has been studied thoroughly by site-directed mutagenesis.[6−10] The before mentioned peptide binding lysine, tyrosine, and glutamate residue are all conserved in YbgH and YjdL, suggesting that peptide binding occurs in the same orientation as observed for the more prototypical peptide transporters.[7−9] The similarity of the YbgH and YjdL binding sites also makes it highly likely that YbgH will transport the dipeptide Ala−Ala in analogy with YjdL.[6] The absence of E_1 and R in the E_1XXE_2R motif suggests a proton coupling mechanism and subsequent structural changes that may differ from the prototypical POTs. It has, however, been shown that the E_2 residue in YbgH (Glu21) and probably also YjdL (Glu20) is the primary site for protonation[9,11,16] and that lysine could interact with E_2 as well.[11] Combined with the knowledge from the prototypical POTs, that is, interaction with the peptide C-terminus,[3,7] it could be hypothesized that lysine has a role in coupling protonation and substrate binding in YbgH/YjdL.

Here, we have studied the immediate environment of protonated and deprotonated E_2 in YbgH and for both of these states, with and without bound dipeptide, using MD simulations. Our results show that lysine (Lys118) prefers to interact with the unprotonated E_2 rather than the substrate peptide C-terminus. However, upon protonation, this interaction is destabilized, and Lys118 interacts with the peptide C-terminus, suggesting that Lys118 acts as a switch to couple protonation and peptide binding.

RESULTS

Our objectives were to investigate the structural effects of protonation, dipeptide binding, and simultaneous binding or absence of both substrates with focus on Glu21 and Lys118. Hence, four simulations were performed: YbgH with protonated/deprotonated Glu21, that is, apo+H/apo−H, and the same structures with the alanyl dipeptide Ala−Ala (AA) docked into the active site, that is, AA+H and AA−H, respectively. YbgH substrate interactions, in particular, interactions of the peptide C-terminus with Glu21 and Lys118, and global conformations of the structures were closely monitored during the simulation. In all simulations, the initial global conformation was identical to that of the crystal structure, that is, inward open. Furthermore, in the case of the apo and protonated structures, no interactions were observed between Lys118 and Glu21; in the case of the AA complexes, a salt bridge between Lys118 and the AA C-terminus was present in the starting structure.

Proton-Dependent Interactions with Substrates. In the apo−H simulations of YbgH, Glu21 quickly formed a salt bridge with Lys118, which was maintained throughout the three simulations (Figure 1A). In the starting conformations for all simulations, no interactions between these residues were observed. Upon protonation of Glu21 and in the absence of AA (apo+H), interactions with Lys118 were less stable and only occasionally within the hydrogen bonding distance with Glu21 during the simulation (Figure 1B). Also, Glu21 was observed to move away from the peptide binding pocket and Lys118 became disordered, compared to apo−H simulation.

DOI: 10.1021/acsomega.8b02131
ACS Omega 2019, 4, 2040−2046

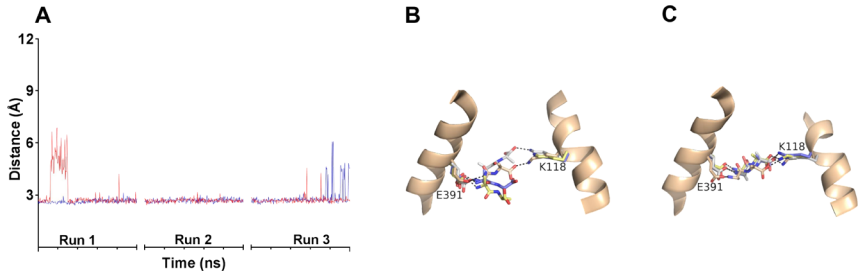

Figure 2. Influence of protonation on substrate binding. (A) Shortest side chain N−O distance (Å) from E391 to Ala−Ala N-terminal as a function of time in AA−H (red) and AA+H (blue). Each run segment corresponds to 100 ns. Overlay of AA binding pose at 0 (wheat), 60 (yellow), 80 (blue), and 100 (white) ns in (B) AA−H and (C) AA+H simulations.

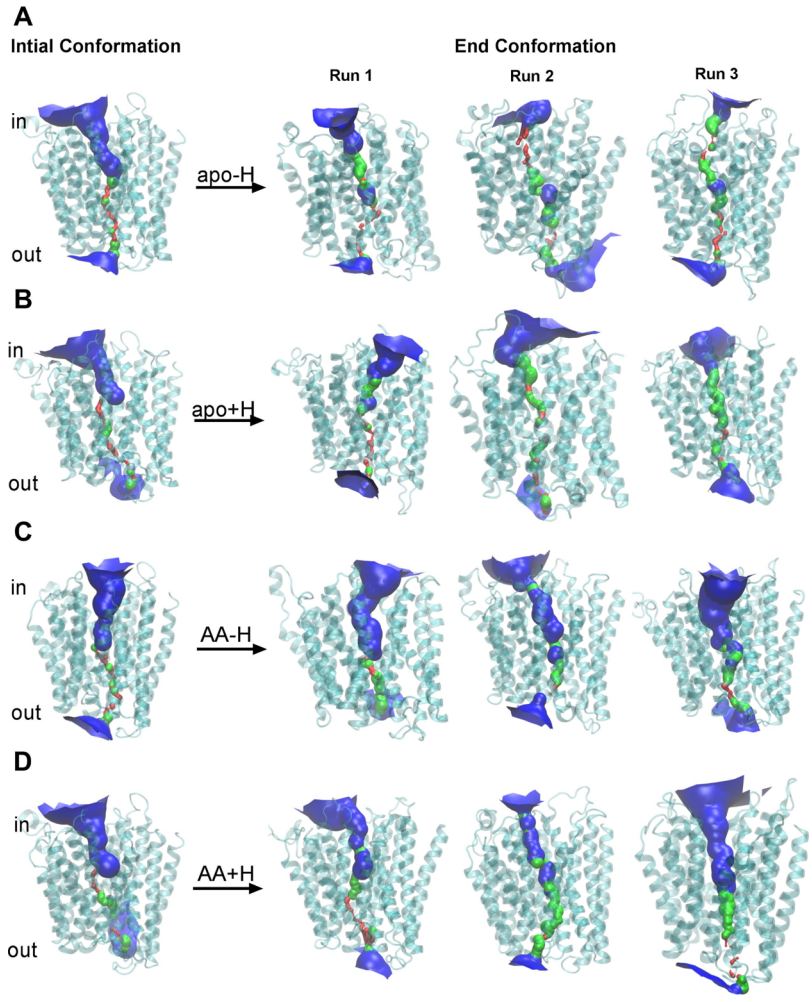

Figure 3. Proton:peptide binding induces conformation changes in YbgH. The structures were analyzed using HOLE (version 2.2), where red, green, and blue represent the pore diameter of <1.2, 1.2−2.30, and >2.30 Å, respectively. This includes (A) apo−H, (B) apo+H, (C) AA−H, and (D) AA+H structures of YbgH, representing transition from initial conformation at 0 ns to end conformations from three individual runs at 100 ns.

Thus, protonation of Glu21 "releases" Lys118. Next, to investigate the effect of substrate binding, the simulation AA−H was undertaken, that is, with AA docked in the binding site. The initial structure used for this simulation showed a salt bridge between Lys118 and the AA C-terminus (Figure 1C) as has been observed in the crystal structures of POTs with bound peptides.[4]

During the simulation, however, Lys118 shifted conformation and formed a salt bridge with Glu21 (Figure 1C). This shows that Lys118 prefers to form a salt bridge with Glu21 rather than with the AA C-terminus. In the fourth simulation AA+H, with both AA and proton bound, Lys118 interactions with Glu21 were absent and Lys118 instead formed a salt bridge with the AA C-terminus (Figure 1D Run 1) or with neither of the carboxylates (partially observed in Run 2 and Run 3) (Figure 1D). The discrepancies observed between the repeated simulations, that is, partial binding, may be due to the fact that AA is a low-affinity substrate for YjdL and hence also for YbgH.[6,12] A similar situation was also observed previously for GK-POT when run with a substrate with low affinity.[17] Taken together, the result indicate that Lys118 interaction with Glu21 is energetically favorable, except when Glu21 is

DOI: 10.1021/acsomega.8b02131
ACS Omega 2019, 4, 2040−2046

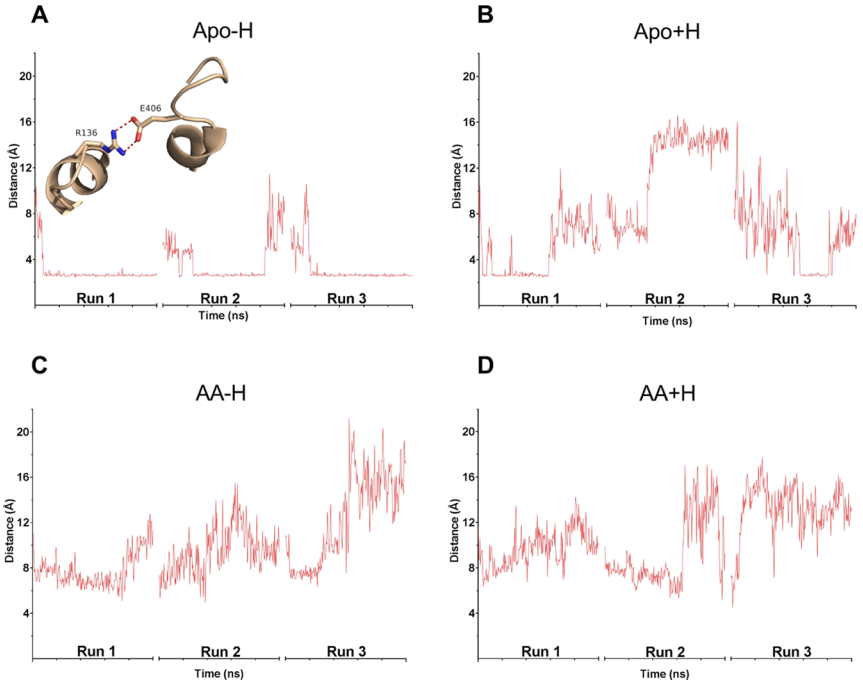

Figure 4. Formation of an intracellular gate in YbgH. The shortest side chain N−O distance (Å) between the gating residues Arg136 and Glu406 (red) as a function of time. (A) apo−H, (B) apo+H, (C) AA−H, and (D) AA+H. Each run segment corresponds to 100 ns. Insets represent the bond distances that were measured.

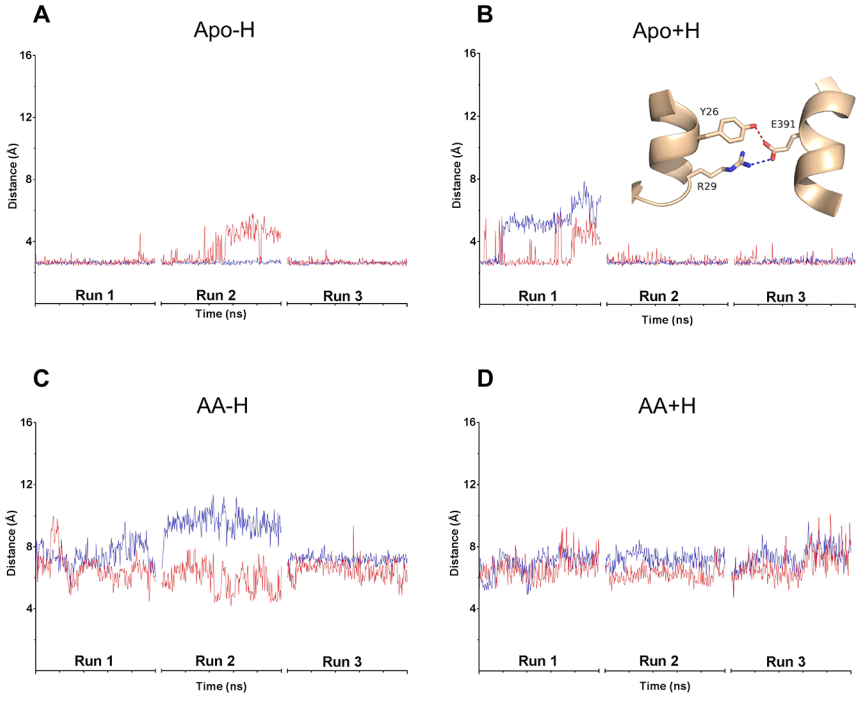

Figure 5. Substrate mimicking interactions facilitate conformational changes in the YbgH apo structure. The shortest side chain N−O distance (Å) from Glu391 to Arg29 (blue) and Tyr26 (red) as a function of time in the simulations of YbgH: (A) apo−H, (B) apo+H, (C) AA−H, and (D) AA +H. Each run segment corresponds to 100 ns. Insets represent the bond distances that were measured.

protonated; when a peptide is present, the interaction between Lys118 and the peptide C-terminus becomes possible. Thus, apparently, Lys118 links Glu21 protonation to peptide binding.

Substrate Binding Stabilized by Protonation. When AA was docked in to the model of YbgH, the binding pose was found to be similar to that observed for the N-terminal and middle alanine residues in the crystal structure of the $PepT_{So2}$:AlaAlaAla complex, PDBID:4TPH.[3] The dipeptide is in an extended conformation and interacts with Lys118 on the N-terminal 6-helix domain and Glu391 in the C-terminal 6-helix domain. First, we examined the position of AA in the AA−H simulation. Here, it was observed that the AA N-terminus is engaged in an interaction with Glu391 (Figure 2A); however, the rest of the dipeptide is quite flexible (Figure

DOI: 10.1021/acsomega.8b02131
ACS Omega 2019, 4, 2040−2046

2B). Contrary to this, in AA+H, when a salt bridge to Lys118 is observed, AA becomes more restrained and stays closer to the starting position (Figure 2C).

Overall Conformational Changes. To investigate the possibility of identifying early events of gate closures/openings, we analyzed the trajectories using HOLE,[31] an approach that has been used in several studies of the dynamics of MFS transporters.[1,32] All initial structures were in an inward-facing conformation, with the periplasmic gates closed (Figure 3). After 100 ns of simulation, YbgH was in an occluded conformation when the transporter was either in the apo state or protonated (Figure 3A,B,D); AA alone or the AA+H-bound structure did not change its overall conformation (Figure 3C). All YbgH occlusions occurred between very quickly (within 10 ns). In the apo state, formation of an intracellular gate between Arg136 and Glu406 was observed (Figure 4); this salt bridge was not seen in the other occluded states.

The occluded structures differ substantially from the nonoccluded ones with respect to the active site pocket. There, helix I undergoes major conformational changes that bring Arg29 and Tyr26 to interaction distance with Glu391 (Figure 5A). This is apparently caused by the absence of AA as Arg29 and Tyr26 show no interaction with Glu391 in the presence of a peptide (Figure 5C,D), and partially overlap with the space that would be occupied with a substrate peptide.

DISCUSSION

In the analysis of the four simulation types, we have focused on Glu21 and Lys118 that are both highly conserved and have been shown to form a charge−charge interaction,[16] an interaction, however, not seen the YbgH crystal structure, probably because of the low pH at crystallization. Glu21 has also been shown to be the site of protonation in YbgH and in other POTs.[9,13,16] Lys118 on the other hand has been shown to interact with the C-terminus of bound peptides in several structures.[4,7] In the apo−H and AA−H simulations, the Glu21/Lys118 salt bridge is rapidly formed, whereas it is never observed in the apo+H and the AA+H simulations. In the AA +H simulation, an interaction between Lys118 and the peptide C-terminus is observed. Thus, Lys118 switches from Glu21 to the peptide C-terminus in a Glu21 protonation-dependent manner. Previously, mutational studies on YjdL, a homologue of YbgH, have shown that Lys118 (Lys117 in YjdL) is not essential for substrate uptake. However, its absence increased the K_t significantly,[7] possibly indicating that Lys118 increases the binding affinity of the substrate. This is in accordance with our observations that when Lys118 is involved in interactions with Glu21, and therefore not interacting with the peptide C-terminus, we observed a higher flexibility of the peptide compared to when Lys118 does interact with the peptide. Taken together, previous and current results show that Lys118 plays a central role in coupling protonation to peptide binding and that Glu21 protonation increases the binding affinity.

The N-terminus of a peptide has been shown to be very important for its affinity toward POTs, even more so than the peptide C-terminus.[33,34] Glu391 and its equivalent in other POTs have been shown to be the counterion for the N-terminus.[2,4,14] We observed strong interactions between the N-terminus and Glu391 in our simulations of AA−H and AA+H. On the other hand, interactions between Lys118 and the C-terminus depended on Glu21 protonation. In the absence of Lys118 to the C-terminus salt bridge, the peptide was found to become disordered while maintaining interaction with E391 most of the time (Figure 2B).

On the basis of all observations, we propose that YbgH peptide binding occurs via a two-step mechanism. First, the peptide is bound in an initial site of the binding pocket via interaction with Glu391. From here, the AA−H simulation show that the peptide temporarily translocates deeper into the binding pocket in proximity of the Glu21−Lys118 salt bridge (Figure 6A). Second, water-mediated[35] protonation of Glu21 releases Lys118 that now interacts with the peptide to form the final complex (Figure 6B). This final complex is very similar to most POT structures with peptides published to date (Figure 6B).

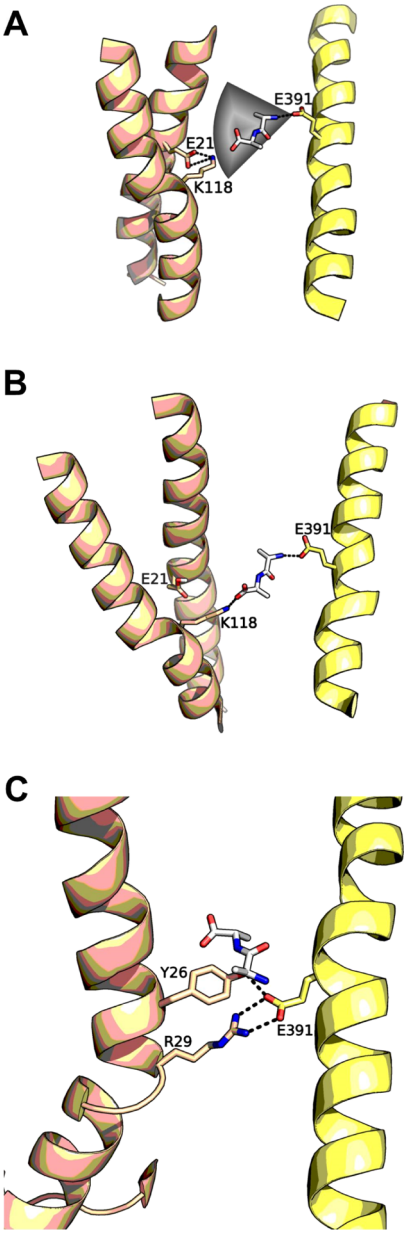

Figure 6. Schematic representation of peptide binding in YbgH, corresponding to the protonation state of Glu21 (A) in the absence and (B) in the presence of proton. (C) Overlay of intramolecular substrate mimicry interactions in YbgH with docked AA. The peptide AA is shown in white and the gray shield represent the flexibility of AA in AA−H simulation.

DOI: 10.1021/acsomega.8b02131
ACS Omega 2019, 4, 2040−2046

MFS transporters undergo conformational changes that expose the substrate binding site to the outside or inside in an alternating fashion. The transition from outward to inward facing and vice versa has to proceed through an occluded conformation, where the substrate binding pocket is inaccessible from either side.[1] What is also noteworthy is that POTs, and many other MFS, can transport protons and peptides from the inside to the outside, given that the proton gradient is reversed.[14,36] For POTs, occluded conformations are only formed either when the transporter has a bound proton and a peptide or when it is inward facing and is empty after substrate release and has to return to the outside. There is an understanding that formation of occluded or other states, within the MFS, is due to movement of transmembrane helices to form constrictions/gates.[1] The opening and closing of these gates is stabilized by the formation or breaking of key salt bridges, which is controlled by the presence or absence of substrate(s).[13,18] Our simulations support this because in apo−H, we observe constrictions that lead to the formation of an occluded YbgH structure stabilized by an intracellular salt bridge between residues Arg136 and Glu406.

A striking observation in the apo−H YbgH binding pocket is that Arg29 and Tyr 26 move significantly in towards and interact with Glu391 through a salt bridge and hydrogen bond, respectively. By this movement, Arg29 and Tyr26 effectively occupy the space that would otherwise be occupied by a bound peptide (Figure 6C). Previously, Arg29 and Glu391 equivalents in other POTs had been proposed to be involved in intramolecular salt bridges that would promote conformational changes, however with other binding partners.[13] We speculate that our finding might be a mechanism of intramolecular substrate mimicking that may explain how an empty transporter moves from the empty inward-facing conformation back to the outward-facing conformation. This type of a mechanism has been observed for the leucine transporter LeuT, where Malinauskaite et al. show that an intramolecular leucine residue occupies the substrate binding pocket to facilitate return to the outward-facing conformation and complete the transport cycle.[37] Similar studies on LacY showed that an apo structure quickly shifted conformation from an inside open to occluded conformation[32,38] as we have observed for apo YbgH.

MATERIALS AND METHODS

Molecular Modeling. The 3D structure of YbgH is available as with PDBID 4Q65.[16] Missing loops were modeled using the Modeller loop-building interface in Chimera (version 1.10.1).[19,20] A total of 100 structures were generated and the model with the highest *Z*-score was used for this study.

Substrate Docking. Schrödinger software (version 2018-1)[21] was used for the protein, ligand, and docking studies. The dipeptide substrate Ala−Ala docked into YbgH. Ala−Ala was prepared using the LigPrep[22] wizard and then subjected to conformational search by default settings in MacroModel.[23] The low-energy conformation structure obtained was used for docking using the program Glide.[24] The model of YbgH was prepared using protein preparation wizard prior to docking.[25] The hydrogen bond assignments were done using PROPKA with default settings at pH of 7.0 and minimized using force field OPLS3.[25] A docking voxel of size 20 Å was generated using a centroid derived from the positions of selected known active site residues such as Lys118, Tyr26, and Glu391 using the Glide Receptor Grid Generation tool. Finally, the ligand Ala−Ala was docked into YbgH using Glide and the docking pose with the highest docking score was used for this study.[24,26−28]

MD Simulations. The protein preparation and minimization procedures were done as described above. The apo or Ala−Ala docked models were used for the simulations. The protonated state of YbgH was generated by the addition of a proton to Glu21, which was negatively charged in the state derived from the PROPKA calculations.[25] To investigate the structural dynamics of YbgH, a full-length structural model was generated using MODELLER as described earlier.[19,20] The system for the MD simulation was created with Desmond system builder using 1-palmitoyl-2-oleoyl-*sn*-glycero-3-phosphoethanolamine and SPC as membrane and water models, respectively. A standard equilibration protocol was used for equilibrating the system. Subsequently, the MD runs were performed with Desmond on GPU using force field OPLS3.[21,29] Each of the simulations were performed for 100 ns in triplicates, with different initial velocities. The intramolecular distances between the residues during the simulation were measured using visual molecular dynamics.[30] To determine the conformational states, we have manually aligned YbgH from the respective MD time frame so that the coordinates of the origin was at the central binding cavity and the *z*-axis was arranged parallel to the membrane. Hole (version 2.2) was then used to determine the maximum pore size along the *z*-axis.[31]

AUTHOR INFORMATION

Corresponding Author

*E-mail: om@sund.ku.dk. Phone: +45 35336175. Fax: +45 35336100 (O.M.).

ORCID

Michael Gajhede: 0000-0001-9864-2287

Flemming Steen Jørgensen: 0000-0001-8040-2998

Osman Mirza: 0000-0001-9435-0690

Notes

The authors declare no competing financial interest.

ACKNOWLEDGMENTS

This research is funded by the Faculty of Health and Medical Sciences, University of Copenhagen, Denmark. R.K.'s stay at the University of Copenhagen, Denmark, was funded by the Higher Education Commission, Pakistan.

REFERENCES

(1) Fowler, P. W.; Orwick-Rydmark, M.; Radestock, S.; Solcan, N.; Dijkman, P. M.; Lyons, J. A.; Kwok, J.; Caffrey, M.; Watts, A.; Forrest, L. R.; Newstead, S. Gating topology of the proton-coupled oligopeptide symporters. *Structure* **2015**, *23*, 290−301.

(2) Martinez Molledo, M.; Quistgaard, E. M.; Flayhan, A.; Pieprzyk, J.; Löw, C. Multispecific Substrate Recognition in a Proton-Dependent Oligopeptide Transporter. *Structure* **2018**, *26*, 467−476.e4.

(3) Guettou, F.; Quistgaard, E. M.; Raba, M.; Moberg, P.; Löw, C.; Nordlund, P. Selectivity mechanism of a bacterial homolog of the human drug-peptide transporters PepT1 and PepT2. *Nat. Struct. Mol. Biol.* **2014**, *21*, 728−731.

(4) Lyons, J. A.; Parker, J. L.; Solcan, N.; Brinth, A.; Li, D.; Shah, S. T.; Caffrey, M.; Newstead, S. Structural basis for polyspecificity in the POT family of proton-coupled oligopeptide transporters. *EMBO Rep.* **2014**, *15*, 886−893.

DOI: 10.1021/acsomega.8b02131
ACS Omega 2019, 4, 2040−2046

(5) Newstead, S. Recent advances in understanding proton coupled peptide transport via the POT family. *Curr. Opin. Struct. Biol.* **2017**, *45*, 17−24.
(6) Prabhala, B. K.; Aduri, N. G.; Jensen, J. M.; Ernst, H. A.; Iram, N.; Rahman, M.; Mirza, O. New insights into the substrate specificities of proton-coupled oligopeptide transporters from E. coli by a pH sensitive assay. *FEBS Lett.* **2014**, *588*, 560−565.
(7) Jensen, J. M.; Aduri, N. G.; Prabhala, B. K.; Jahnsen, R.; Franzyk, H.; Mirza, O. Critical role of a conserved transmembrane lysine in substrate recognition by the proton-coupled oligopeptide transporter YjdL. *Int. J. Biochem. Cell Biol.* **2014**, *55*, 311−317.
(8) Jensen, J. M.; Ismat, F.; Szakonyi, G.; Rahman, M.; Mirza, O. Probing the putative active site of YjdL: an unusual proton-coupled oligopeptide transporter from E. coli. *PLoS One* **2012**, *7*, No. e47780.
(9) Jensen, J. M.; Ernst, H. A.; Wang, X.; Hald, H.; Ditta, A. C.; Ismat, F.; Rahman, M.; Mirza, O. Functional investigation of conserved membrane-embedded glutamate residues in the proton-coupled peptide transporter YjdL. *Protein Pept. Lett.* **2012**, *19*, 282−287.
(10) Jensen, J. M.; Simonsen, F. C.; Mastali, A.; Hald, H.; Lillebro, I.; Diness, F.; Olsen, L.; Mirza, O. Biophysical characterization of the proton-coupled oligopeptide transporter YjdL. *Peptides* **2012**, *38*, 89−93.
(11) Aduri, N. G.; Prabhala, B. K.; Ernst, H. A.; Jørgensen, F. S.; Olsen, L.; Mirza, O. Salt Bridge Swapping in the EXXERFXYY Motif of Proton-coupled Oligopeptide Transporters. *J. Biol. Chem.* **2015**, *290*, 29931−29940.
(12) Ernst, H. A.; Pham, A.; Hald, H.; Kastrup, J. S.; Rahman, M.; Mirza, O. Ligand binding analyses of the putative peptide transporter YjdL from E. coli display a significant selectivity towards dipeptides. *Biochem. Biophys. Res. Commun.* **2009**, *389*, 112−116.
(13) Solcan, N.; Kwok, J.; Fowler, P. W.; Cameron, A. D.; Drew, D.; Iwata, S.; Newstead, S. Alternating access mechanism in the POT family of oligopeptide transporters. *EMBO J.* **2012**, *31*, 3411−3421.
(14) Guettou, F.; Quistgaard, E. M.; Trésaugues, L.; Moberg, P.; Jegerschöld, C.; Zhu, L.; Jong, A. J. O.; Nordlund, P.; Löw, C. Structural insights into substrate recognition in proton-dependent oligopeptide transporters. *EMBO Rep.* **2013**, *14*, 804−810.
(15) Newstead, S.; Drew, D.; Cameron, A. D.; Postis, V. L. G.; Xia, X.; Fowler, P. W.; Ingram, J. C.; Carpenter, E. P.; Sansom, M. S. P.; McPherson, M. J.; Baldwin, S. A.; Iwata, S. Crystal structure of a prokaryotic homologue of the mammalian oligopeptide-proton symporters, PepT1 and PepT2. *EMBO J.* **2010**, *30*, 417−426.
(16) Zhao, Y.; Mao, G.; Liu, M.; Zhang, L.; Wang, X.; Zhang, X. C. Crystal structure of the E. coli peptide transporter YbgH. *Structure* **2014**, *22*, 1152−1160.
(17) Immadisetty, K.; Hettige, J.; Moradi, M. What Can and Cannot Be Learned from Molecular Dynamics Simulations of Bacterial Proton-Coupled Oligopeptide Transporter GkPOT? *J. Phys. Chem. B* **2016**, *121*, 3644−3656.
(18) Doki, S.; Kato, H. E.; Solcan, N.; Iwaki, M.; Koyama, M.; Hattori, M.; Iwase, N.; Tsukazaki, T.; Sugita, Y.; Kandori, H.; Newstead, S.; Ishitani, R.; Nureki, O. Structural basis for dynamic mechanism of proton-coupled symport by the peptide transporter POT. *Proc. Natl. Acad. Sci. U. S. A.* **2013**, *110*, 11343−11348.
(19) Pettersen, E. F.; Goddard, T. D.; Huang, C. C.; Couch, G. S.; Greenblatt, D. M.; Meng, E. C.; Ferrin, T. E. UCSF Chimera?A visualization system for exploratory research and analysis. *J. Comput. Chem.* **2004**, *25*, 1605−1612.
(20) Webb, B.; Sali, A. Comparative Protein Structure Modeling Using MODELLER. *Curr. Protoc. Bioinf.* **2014**, *47*, 5.6.1−5.6.32.
(21) *Schrödinger*, 2018-1; LLC: New York, NY, 2018.
(22) *Schrödinger*, Release 2018-1; LigPrep, Schrödinger, LLC: New York, NY, 2018.
(23) *Schrödinger*, Release 2018-1; MacroModel, Schrödinger, LLC: New York, NY, 2018.
(24) *Schrödinger*, Release 2018-1; Glide, Schrödinger, LLC: New York, NY, 2018.
(25) *Schrödinger Suite 2018-1 Protein Preparation Wizard*; Epik, Schrödinger, LLC, New York, NY, 2016; Impact, Schrödinger, LLC, New York, NY, 2016; Prime, Schrödinger, LLC: New York, NY, 2018.
(26) Halgren, T. A.; Murphy, R. B.; Friesner, R. A.; Beard, H. S.; Frye, L. L.; Pollard, W. T.; Banks, J. L. Glide: a new approach for rapid, accurate docking and scoring. 2. Enrichment factors in database screening. *J. Med. Chem.* **2004**, *47*, 1750−1759.
(27) Friesner, R. A.; Banks, J. L.; Murphy, R. B.; Halgren, T. A.; Klicic, J. J.; Mainz, D. T.; Repasky, M. P.; Knoll, E. H.; Shelley, M.; Perry, J. K.; Shaw, D. E.; Francis, P.; Shenkin, P. S. Glide: a new approach for rapid, accurate docking and scoring. 1. Method and assessment of docking accuracy. *J. Med. Chem.* **2004**, *47*, 1739−1749.
(28) Friesner, R. A.; Murphy, R. B.; Repasky, M. P.; Frye, L. L.; Greenwood, J. R.; Halgren, T. A.; Sanschagrin, P. C.; Mainz, D. T. Extra Precision Glide: Docking and Scoring Incorporating a Model of Hydrophobic Enclosure for Protein−Ligand Complexes. *J. Med. Chem.* **2006**, *49*, 6177−6196.
(29) *Desmond Molecular Dynamics System*, D. E. Shaw Research, New York, NY, 2018; Maestro-Desmond Interoperability Tools, Schrödinger: New York, NY, 2018.
(30) Humphrey, W.; Dalke, A.; Schulten, K. VMD: visual molecular dynamics. *J. Mol. Graphics* **1996**, *14*, 33−38.
(31) Smart, O. S.; Neduvelil, J. G.; Wang, X.; Wallace, B. A.; Sansom, M. S. P. HOLE: a program for the analysis of the pore dimensions of ion channel structural models. *J. Mol. Graphics* **1996**, *14*, 354−360.
(32) Stelzl, L. S.; Fowler, P. W.; Sansom, M. S. P.; Beckstein, O. Flexible gates generate occluded intermediates in the transport cycle of LacY. *J. Mol. Biol.* **2014**, *426*, 735−751.
(33) Fang, G.; Konings, W. N.; Poolman, B. Kinetics and substrate specificity of membrane-reconstituted peptide transporter DtpT of Lactococcus lactis. *J. Bacteriol.* **2000**, *182*, 2530−2535.
(34) Meredith, D.; Temple, C. S.; Guha, N.; Sword, C. J.; Boyd, C. A. R.; Collier, I. D.; Morgan, K. M.; Bailey, P. D. Modified amino acids and peptides as substrates for the intestinal peptide transporter PepT1. *Eur. J. Biochem.* **2000**, *267*, 3723−3728.
(35) Parker, J. L.; Li, C.; Brinth, A.; Wang, Z.; Vogeley, L.; Solcan, N.; Ledderboge-Vucinic, G.; Swanson, J. M. J.; Caffrey, M.; Voth, G. A.; Newstead, S. Proton movement and coupling in the POT family of peptide transporters. *Proc. Natl. Acad. Sci. U.S.A.* **2017**, *114*, 13182−13187.
(36) Irie, M.; Terada, T.; Okuda, M.; Inui, K.-i. Efflux properties of basolateral peptide transporter in human intestinal cell line Caco-2. *Pflugers Arch.* **2004**, *449*, 186−194.
(37) Malinauskaite, L.; Said, S.; Sahin, C.; Grouleff, J.; Shahsavar, A.; Bjerregaard, H.; Noer, P.; Severinsen, K.; Boesen, T.; Schiøtt, B.; Sinning, S.; Nissen, P. A conserved leucine occupies the empty substrate site of LeuT in the Na(+)-free return state. *Nat. Commun.* **2016**, *7*, 11673.
(38) Holyoake, J.; Sansom, M. S. P. Conformational change in an MFS protein: MD simulations of LacY. *Structure* **2007**, *15*, 873−884.

DOI: 10.1021/acsomega.8b02131
ACS Omega 2019, 4, 2040−2046